Chemical Science

ROYAL SOCIETY OF CHEMISTRY

EDGE ARTICLE

View Article Online
View Journal | View Issue

Cite this: *Chem. Sci.*, 2023, **14**, 11499

All publication charges for this article have been paid for by the Royal Society of Chemistry

Cyclobutane-bearing restricted anchoring residues enabled geometry-specific hydrocarbon peptide stapling†

Baobao Chen,‡[a] Chao Liu,‡[a] Wei Cong,[a] Fei Gao,[a] Yan Zou,[b] Li Su,[a] Lei Liu,[c] Alexander Hillisch,[de] Lutz Lehmann,[d] Donald Bierer,[d] Xiang Li*[b] and Hong-Gang Hu*[a]

Stapled peptides are regarded as the promising next-generation therapeutics because of their improved secondary structure, membrane permeability and metabolic stability as compared with the prototype linear peptides. Usually, stapled peptides are obtained by a hydrocarbon stapling technique, anchoring from paired olefin-terminated unnatural amino acids and the consequent ring-closing metathesis (RCM). To investigate the adaptability of the rigid cyclobutane structure in RCM and expand the chemical diversity of hydrocarbon peptide stapling, we herein described the rational design and efficient synthesis of cyclobutane-based conformationally constrained amino acids, termed (*E*)-1-amino-3-(but-3-en-1-yl) cyclobutane-1-carboxylic acid (E_7) and (*Z*)-1-amino-3-(but-3-en-1-yl)cyclobutane-1-carboxylic acid (Z_7). All four combinations including E_7-E_7, E_7-Z_7, Z_7-Z_7 and Z_7-E_7 were proven to be applicable in RCM-mediated peptide stapling to afford the corresponding geometry-specific stapled peptides. With the aid of the combined quantum and molecular mechanics, the E_7-E_7 combination was proven to be optimal in both the RCM reaction and helical stabilization. With the spike protein of SARS-CoV-2 as the target, a series of cyclobutane-bearing stapled peptides were obtained. Among them, E_7-E_7 geometry-specific stapled peptides indeed exhibit higher α-helicity and thus stronger biological activity than canonical hydrocarbon stapled peptides. We believe that this methodology possesses great potential to expand the scope of the existing peptide stapling strategy. These cyclobutane-bearing restricted anchoring residues served as effective supplements for the existing olefin-terminated unnatural amino acids and the resultant geometry-specific hydrocarbon peptide stapling provided more potential for peptide therapeutics.

Received 16th August 2023
Accepted 28th September 2023

DOI: 10.1039/d3sc04279k

rsc.li/chemical-science

Introduction

Protein–protein interactions (PPIs) regulate several signaling pathways and physiological processes,[1–4] and dysfunction of these interactions is thought to be associated with many human diseases.[5–7] Therefore, targeting specific protein–protein interactions to achieve the treatment of related diseases is currently a research hotspot in drug design.[8–11] Benefiting from their unique physiochemical properties including the flexible backbone structure and a molecular size between those of small molecules and biomacromolecules (proteins and antibodies), peptides are regarded as suitable candidates for modulating or interfering with PPIs.[12,13] However, linear peptides are rarely able to spontaneously form stable secondary structures (mostly helices) in solution, resulting in poor *in vivo* stability and membrane impermeability, which represent major stumbling blocks for peptide drug development.[14–16]

Currently, the most straightforward and effective chemical modification to stabilize peptide helices is the peptide stapling strategy. It refers to the concept of peptide side-chain cross-linking *via* the peptidic or non-peptidic structure, such as disulfide surrogates,[17–19] lactams,[20,21] triazole,[22–24] and other compounds,[25,26] to preorganize a stable helical conformation with a reduced entropic penalty. Stapling strategies such as *via* dithiocarbamate[27] (DTC), formaldehyde crosslinking,[28] sulfonamide[29] and other stapling strategies[16,30–34] were recently developed, which successfully improved the physicochemical and pharmacological properties of linear peptides. Among these stapling strategies, the all-hydrocarbon stapling strategy developed by Verdine and co-workers[35] is regarded as the most

[a]*School of Medicine or Institute of Translational Medicine, Shanghai University, Shanghai 200444, China. E-mail: hhu66@shu.edu.cn*

[b]*School of Pharmacy, Second Military Medical University, Shanghai 200433, China. E-mail: xiangli@smmu.edu.cn*

[c]*Department of Chemistry, Tsinghua University, Beijing 100084, China*

[d]*Bayer AG, Pharma Division, Drug Discovery Sciences, Aprather Weg 18A, Wuppertal 42096, Germany*

[e]*UCB BioSciences GmbH, Alfred-Nobel-Straße 10, 40789 Monheim am Rhein, Germany*

† Electronic supplementary information (ESI) available. See DOI: https://doi.org/10.1039/d3sc04279k

‡ These authors contributed to this work equally.

established one and has been applied in inhibiting diverse PPIs.[36–38] The *i*, *i* + 4 position side-chain cross-linking was realized *via* the Grubbs reagent-catalyzed ring-closing metathesis (RCM) reaction between olefin-bearing amino acids *S*-2-(4-pentenyl)Ala-OH ($\mathbf{S_5}$) and/or *R*-2-(4-pentenyl)Ala-OH ($\mathbf{R_5}$). A notable example was ALRN-6924, an all-hydrocarbon stapled peptide antagonist of both MDM2 and MDMX, which reactivated the p53 pathway to kill tumor cells and has entered Phase 2 trials for advanced solid tumors and lymphomas.[39] Another important case is the stapled peptide developed by Axel T Brunger's team, which was proven to be capable of treating the inability to control mucus in the respiratory tract.[40] Peptide stapling has solved the druggability problem of peptide drugs to some extent. However, to expand the chemical diversity and continue investigating their potential, more stapling blocks with different chemical structures are still highly advantageous. For example, our research group has developed a series of new stapling amino acids containing natural amino acid side chains that can be used in the standard stapling chemistry of stable α-helical conformation peptides[41] (Fig. 1A).

Recently, cyclobutane-based conformationally constrained amino acids have been successfully used in solid-state NMR spectroscopy studies to determine the structure, alignment, and dynamics of membrane-bound peptides under quasi-native conditions.[42–44] These unnatural amino acids are similar to the natural amino acids in steric size, polarity, ionizability, and conformational propensities, which may not perturb the native structure or function of peptides. Additionally, they are highly compatible with the standard procedures of peptide synthesis. Most importantly, the cyclobutane-based conformationally constrained structure ensures that the ^{19}F reporter group is in a geometrically well-defined position relative to the peptide backbone.[45] Because one of the important goals of peptide stapling is to restrict peptide backbone conformations, it remains interesting to explore whether these conformationally constrained amino acids may provide more rigid structures in stapled peptide development, resulting in better pharmacological activities.

As presented in Fig. 1B, we described herein the rational design and synthesis of novel cyclobutane-bearing restricted anchoring residues, termed (*E*)-1-amino-3-(but-3-en-1-yl) cyclobutane-1-carboxylic acid ($\mathbf{E_7}$) and (*Z*)-1-amino-3-(but-3-en-1-yl)cyclobutane-1-carboxylic acid ($\mathbf{Z_7}$). Both and either $\mathbf{E_7}$ and $\mathbf{Z_7}$ could be used in RCM-mediated hydrocarbon peptide stapling. Four geometry-specific stapled peptides involving $\mathbf{E_7}$-$\mathbf{E_7}$, $\mathbf{E_7}$-$\mathbf{Z_7}$, $\mathbf{Z_7}$-$\mathbf{Z_7}$ and $\mathbf{Z_7}$-$\mathbf{E_7}$ combinations were obtained, of which the $\mathbf{E_7}$-$\mathbf{E_7}$ combination was proven to be optimal in the RCM reaction according to both *in silico* and on-resin experiments. Therefore, combining quantum and molecular mechanics, we demonstrated that the $\mathbf{E_7}$-$\mathbf{E_7}$ combination exhibited the highest helical content in secondary structural stabilization. A series of cyclobutane-bearing stapled peptides, with the spike protein of SARS-CoV-2 as the target, were obtained and $\mathbf{E_7}$-$\mathbf{E_7}$ geometry-specific stapled peptides were proven to display the highest α-helicity and best biological activities among varying isomers.

Results and discussion

As presented in Scheme 1, the chemical synthesis of $\mathbf{E_7}$ and $\mathbf{Z_7}$ was completed using the commercially available hex-5-en-1-ol (**3**) as the starting material. In general, benzyl protection was easily implemented on hydroxyl group **3** with the treatment of NaH and BnBr to provide compound **4**. Ketone **5** was obtained from compound **4** *via* a [2 + 2] cycloaddition with dichloroketene

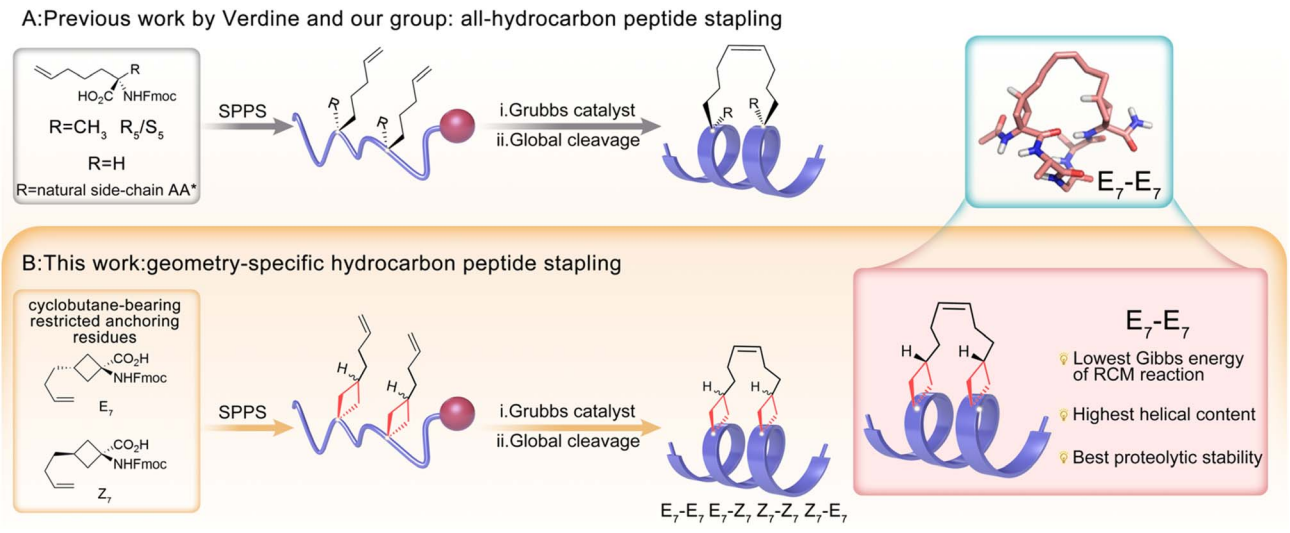

Fig. 1 (A) Previous all-hydrocarbon peptide stapling strategies anchoring from $\mathbf{S_5}$, $\mathbf{R_5}$ or AA* with natural side-chains developed by Verdine and our groups. The cyclization procedure was performed with the aid of Grubbs reagent-catalyzed ring-closing metathesis (RCM) reaction. (B) Cyclobutane-bearing restricted anchoring residues $\mathbf{E_7}$ and $\mathbf{Z_7}$ were rationally designed and synthesized. Similar RCM reactions were applicable for geometry-specific hydrocarbon peptide stapling, to afford four varying stapled peptides involving $\mathbf{E_7}$-$\mathbf{E_7}$, $\mathbf{E_7}$-$\mathbf{Z_7}$, $\mathbf{Z_7}$-$\mathbf{Z_7}$ and $\mathbf{Z_7}$-$\mathbf{E_7}$ paired residues. The $\mathbf{E_7}$-$\mathbf{E_7}$ combination involving stapled peptide was proven to be optimal, exhibiting the lowest Gibbs energy of the RCM reaction, the highest helical content and the best proteolytic stability.

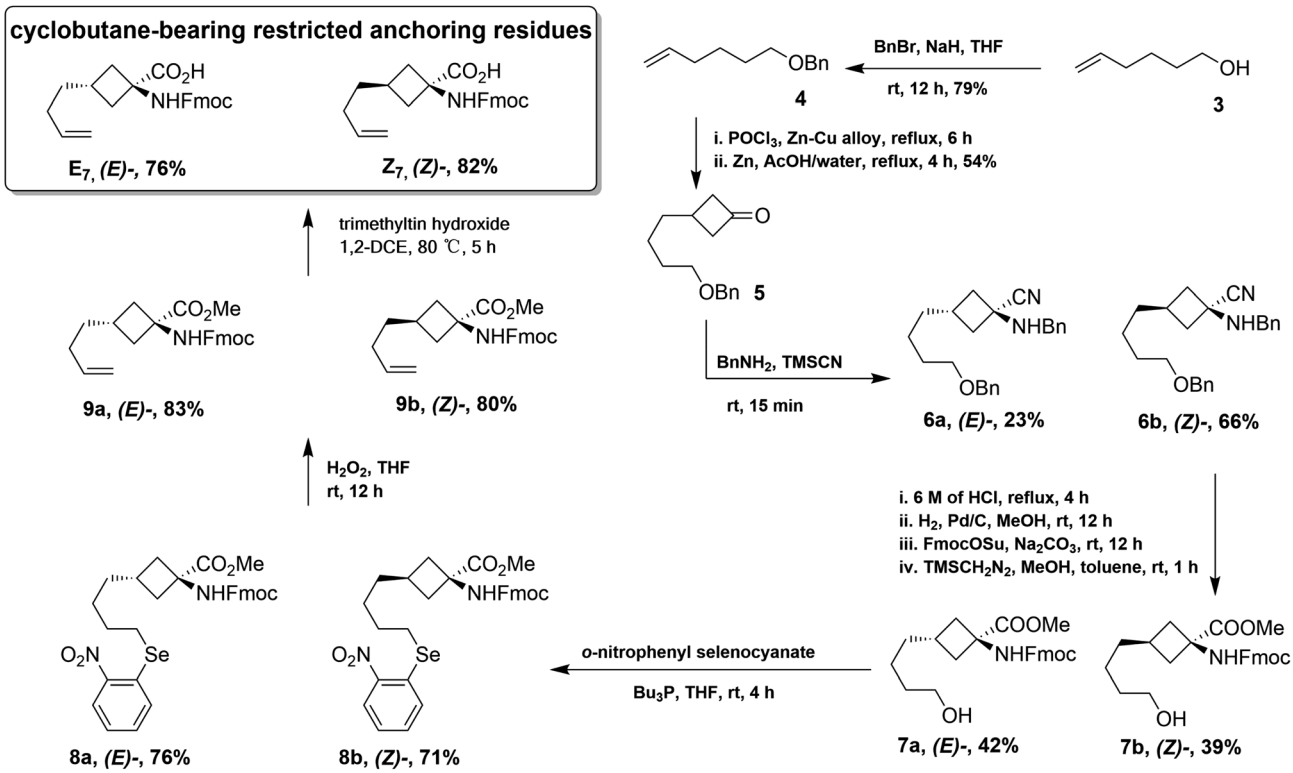

Scheme 1 The synthetic route of cyclobutane-bearing restricted anchoring residues E_7 and Z_7.

generated *in situ* from trichloroacetyl chloride and a copper–zinc alloy and following a hydrogenation reaction catalyzed by zinc powder in acetic acid. The following Strecker reaction with benzylamine and trimethylsilyl cyanide (TMSCN) provided aminonitrile **6** as a 3 : 1 mixture of stereoisomers that were easily separated by column chromatography on silica gel. **6a** and **6b** were then subjected to acidic hydrolysis with 6 M hydrochloric acid. The following Pd-catalyzed hydrogenolysis of the benzyl protection, *N*-Fmoc protection with Fmoc-OSu, and treatment with (trimethylsilyl)diazomethane provided compounds **7a** and **7b**. To perform the Grieco–Sharpless olefination reaction, **7a** and **7b** were reacted with *o*-nitrophenyl selenocyanate and tributylphosphine to yield **8a** and **8b**, and the subsequent elimination transformed **8a** and **8b** into the olefinic intermediates **9a** and **9b**, respectively, *via* the oxidation of hydrogen peroxide. Finally, selective deprotection of methyl esters was realized with the treatment of trimethyltin hydroxide to provide target amino acids $\mathbf{E}_7$ and $\mathbf{Z}_7$ whose absolute geometries were confirmed by following NOESY experiments (Fig. S1†).

With $\mathbf{E}_7$ and $\mathbf{Z}_7$ in hand, our next plan was to perform the RCM-mediated peptide stapling on resin. Either $\mathbf{E}_7$ or $\mathbf{Z}_7$ could be introduced at *i*, *i* + 4 space, representing four varying combinations. Density functional theory (DFT)-based theoretical calculation was first performed to explore the RCM reaction involving different combinations of $\mathbf{E}_7$ and $\mathbf{Z}_7$, starting from Ac-$\mathbf{E}_7$/$\mathbf{Z}_7$-Ala-Gly-Ala-$\mathbf{E}_7$/$\mathbf{Z}_7$-NH_2 peptide sequences. As presented in Fig. 2A, the Gibbs free energies ($\Delta_r G_m$) of the four combinations of RCM reactions were −1.76, 0.24, 0.43 and −0.50 kcal mol^{-1}, respectively. According to the thermodynamic principle, the more negative the $\Delta_r G_m$, the easier it was to perform the reaction, resulting in more stable products. Therefore, it could be predicted that, compared with those of $\mathbf{E}_7$-$\mathbf{Z}_7$ and $\mathbf{Z}_7$-$\mathbf{Z}_7$ combinations, the RCM reactions of $\mathbf{E}_7$-$\mathbf{E}_7$ and $\mathbf{Z}_7$-$\mathbf{E}_7$ combinations were easier to perform and the former combination serves as the optimal one.

With the *in silico* energetic analysis as the reference, we next synthesized four stapled peptides through solid-phase peptide synthesis (SPPS) anchoring from cyclobutane-bearing restricted $\mathbf{E}_7$ and $\mathbf{Z}_7$ (Fig. 2B). $\mathbf{E}_7$ and $\mathbf{Z}_7$ were introduced into the peptide backbone using *O*-(6-chloro-1-hydroxybenzotriazol-1-yl)-1,1,3,3-tetramethyluronium hexafluorophosphate (HCTU)/*N*,*N*-diisopropylethylamine (DIPEA) coupling reagents to obtain on-resin linear peptides (on-resin **1a–d**). Then first generation of the Grubbs reagent enabled the RCM reaction to provide on-resin intermediates (on-resin **2a–d**). Finally, crude target peptides **2a–d** with different combinations ($\mathbf{E}_7$-$\mathbf{E}_7$, $\mathbf{E}_7$-$\mathbf{Z}_7$, $\mathbf{Z}_7$-$\mathbf{Z}_7$ and $\mathbf{Z}_7$-$\mathbf{E}_7$) were successfully obtained after cleavage and global deprotection in the presence of trifluoroacetic acid (TFA)/H_2O/triisopropylsilane (TIPs). Subsequent analysis and identification *via* high performance liquid chromatography (HPLC) and mass spectrometry (MS) demonstrated that all the macrocyclization processes were completed with satisfactory conversion rates (84–95%). After purification by semi-preparative reversed-phase HPLC, geometry-specific stapled peptides **2a–d** were obtained in high isolated yields from 24% to 38% (Fig. 2C). Notably, **2a** was obtained with the highest conversion (95%) and isolated yield (38%), consistent with the theoretical calculation results. The above results demonstrated that these

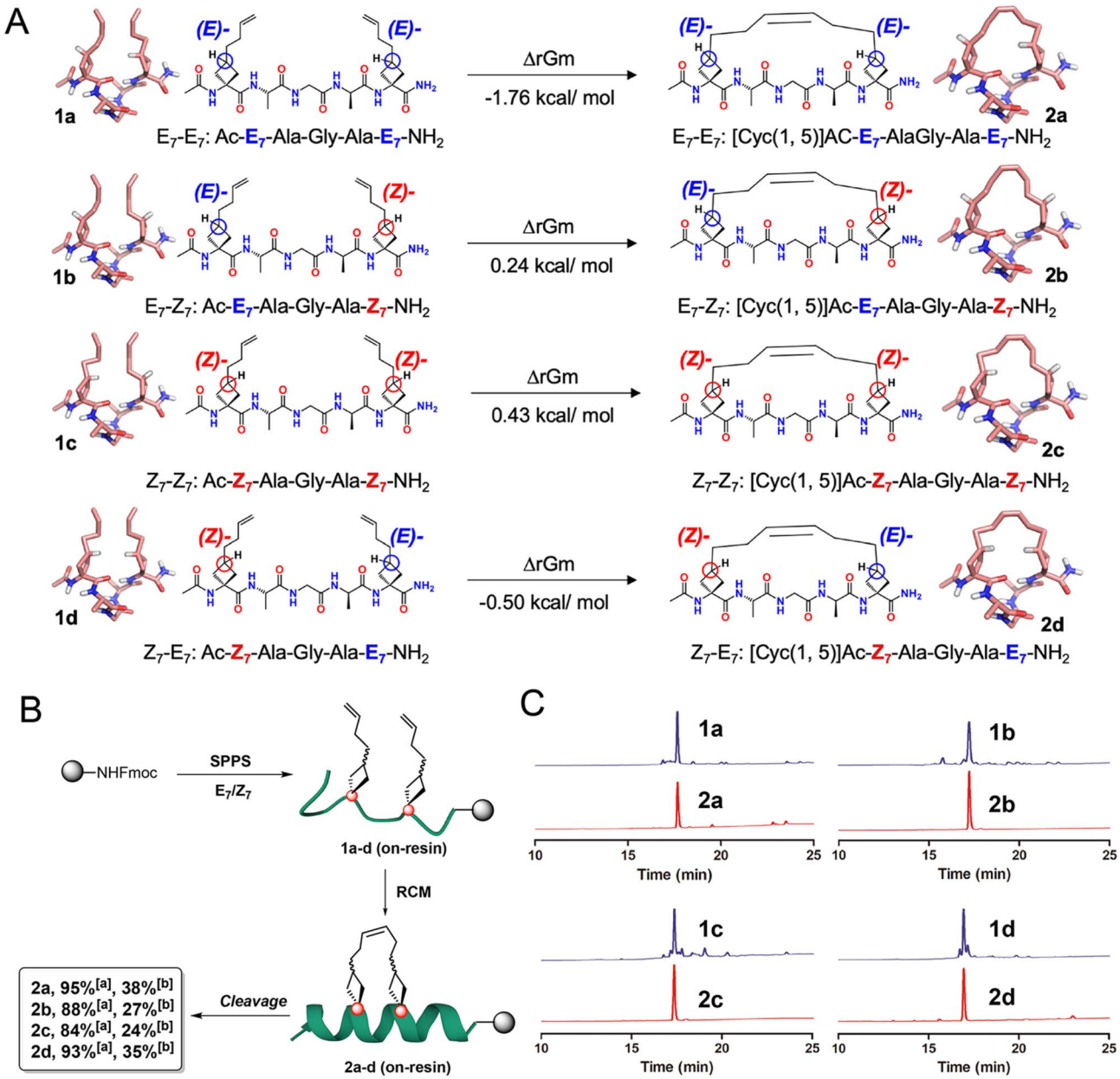

Fig. 2 Geometry-specific hydrocarbon stapled peptides were generated by combining E_7-E_7, E_7-Z_7, Z_7-Z_7 and Z_7-E_7 paired residues and the consequent RCM reaction. (A) The substrates Ac-E_7/Z_7-Ala-Gly-Ala-E_7/Z_7-NH_2 and the stapled peptides products from the RCM reaction and their theoretical Gibbs free energy obtained by density functional theory (DFT). E_7-E_7 was proven as the best combination. (B) The synthesis route of geometry-specific stapled peptides **2a–2d**. [a] The conversions were calculated based on the RCM reaction. [b] The yields represented the overall isolated yields starting from the first-step resin loading. (C) The crude and purified analytic HPLC traces of **2a–2d**. It was confirmed that E_7-E_7 was the optimal combination with the highest conversion, which was consistent with the results of DFT.

cyclobutane-bearing restricted anchoring residues were efficient for generating the geometry-specific and hydrocarbon stapled peptides, and the involving RCM reactions were highly compatible with SPPS.

After verification of the operability of $\mathbf{E}_7$ and $\mathbf{Z}_7$ for RCM-mediated peptide stapling, the next step is to evaluate their ability to stabilize the secondary structure of these geometry-specific stapled peptides. SARS-CoV-2 is highly pathogenic and infectious. The acute respiratory disease pandemic that started in 2019 has seriously endangered human public safety.[46,47] The formation of 6-HB (HR1–HR2 complex) during spike protein-mediated membrane fusion can be used as a conserved and potential target for the design of fusion inhibitors.[48,49] Therefore, we selected our team's previously developed stapled SEK1-12 peptide (unpublished data), which targets the HR1 domain of the SARS-CoV-2 spike protein, as a template peptide. We constructed and efficiently obtained the stapled peptides SEK1-12-1, SEK1-12-2, SEK1-12-3 and SEK1-12-4 using cyclobutane-bearing restricted anchoring residues $\mathbf{E}_7$ and/or $\mathbf{Z}_7$ (Fig. 3A).

A

Peptide	Sequence	Predicted α-Helicity (%)	Distance (Å)	Pitch (Å)	Area (Å²)
EK1	Ac-SLDQINVTFLDLEYEMKKLEEAIKKLEESYIDLKEL-NH_2	33.5	-	5.2	-
SEK1-12	[Cyc(21, 25)] Ac-SLDQINVTFLDLEYEMKKLES_5AIKS_5LEESYIDLKEL-NH_2	47.1	6.6	5.4	17.8
SEK1-12-1	[Cyc(21, 25)] Ac-SLDQINVTFLDLEYEMKKLEE_7AIKE_7LEESYIDLKEL-NH_2	54.5	6.5	6.1	22.4
SEK1-12-2	[Cyc(21, 25)] Ac-SLDQINVTFLDLEYEMKKLEE_7AIKZ_7LEESYIDLKEL-NH_2	50.9	6.3	5.6	22.1
SEK1-12-3	[Cyc(21, 25)] Ac-SLDQINVTFLDLEYEMKKLEZ_7AIKZ_7LEESYIDLKEL-NH_2	45.4	6.1	5.5	21.5
SEK1-12-4	[Cyc(21, 25)] Ac-SLDQINVTFLDLEYEMKKLEZ_7AIKE_7LEESYIDLKEL-NH_2	44.3	5.6	5.6	21.2

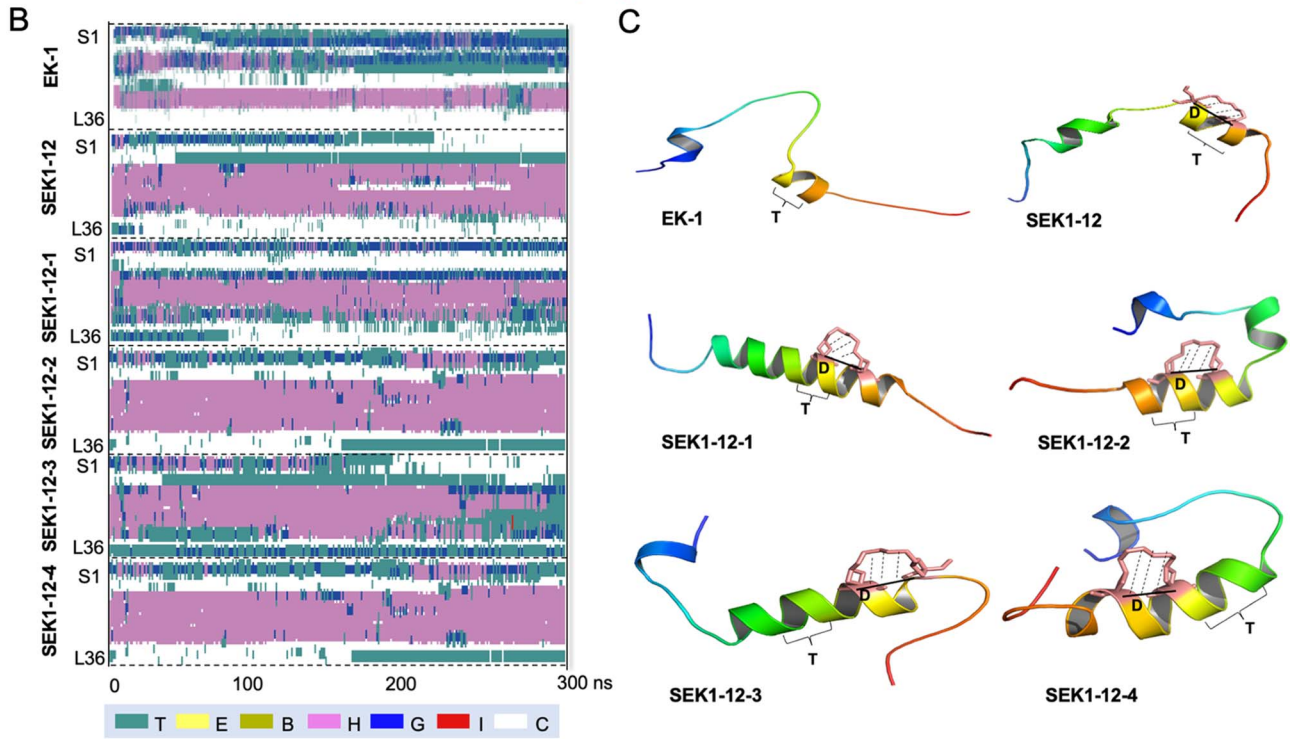

Fig. 3 Theoretical calculation prediction of stapled peptides. (A) Sequence diagrams of stapled peptides with theoretical predictions. (B) The change of the secondary structure of stapled peptides with simulation time. T: hydrogen bond angle; E: parallel beta fold; B: residue within the independent beta bridge; H: α-helical; G: 310-helical; I: π-helical; C: random crimp. (C) Schematic diagram of the three-dimensional structure of the EK1 and its stapled peptides, where *D* represents the anchor distance and *T* represents the pitch.

Based on reasonable stapled peptide structures, the helicity of the six peptides was analyzed in detail by using long time molecular dynamics simulations. Fig. 3B shows the change of the secondary structure of stapled peptides with simulation time after quantum mechanics optimization. There is a great difference in helicity distribution among the six systems, and the order from high to low is SEK1-12-1 > SEK1-12-2 > SEK1-12 > SEK1-12-3 > SEK1-12-4 > EK1. Specifically, SEK1-12-1 and SEK1-12-2 both can maintain the screw well: anchor distance *D* and pitch *T* both are distributed in an optimal range, and the abduction area *S* was the largest, which is more flexibility and conducive to promoting the stability of the screw (Fig. 3C). In terms of SEK1-12-3 and SEK1-12-4, only one of the *D* and *T* parameters is in the appropriate range, and the abduction area *S* is also relatively small, which results in unstable screw with low helicity. The abduction area *S* of SEK1-12 decreased significantly, but the spiral stability was actually higher than that of SEK1-12-3 and SEK1-12-4, which may be related to the replacement of cyclobutane at the anchor point. Compared with EK-1, the other five systems (SEK1-12, SEK1-12-1, SEK1-12-2, SEK1-12-3 and SEK1-12-4) all contain a stapled structure, and the helicity has been greatly improved as expected. To sum up, the helicity of stapled peptides is related to many factors, such as fatty linker and chirality, affecting the distance *D* between anchoring residues, the helix pitch *T*, and the abducting area *S*. These predictive results theoretically suggested that some of these geometry-specific hydrocarbon stapled peptides may provide better secondary structure stability than the classical all-hydrocarbon stapled peptides, which motivated us to perform a follow-up in-depth exploration.

As such, all EK1-derived stapled peptides were successfully synthesized with efficient yields (26–32%). Then, their secondary structures were analyzed by circular dichroism (CD) experiments (Fig. 4A and B). The results indicated that the linear peptide EK1 exhibited a weak helical conformation with a helicity of 13.6%. It has been reported that the α-methyl group

A

Peptide	α-Helicity (%)	$T_{1/2}$ (h)	IC_{50} (μM)
EK-1	13.6	3.2	91.8
SEK1-12	41.5	9.4	6.3
SEK1-12-1	59.2	>12.0	3.5
SEK1-12-2	43.4	10.3	19.2
SEK1-12-3	39.8	7.7	3.5
SEK1-12-4	36.2	8.7	5.1

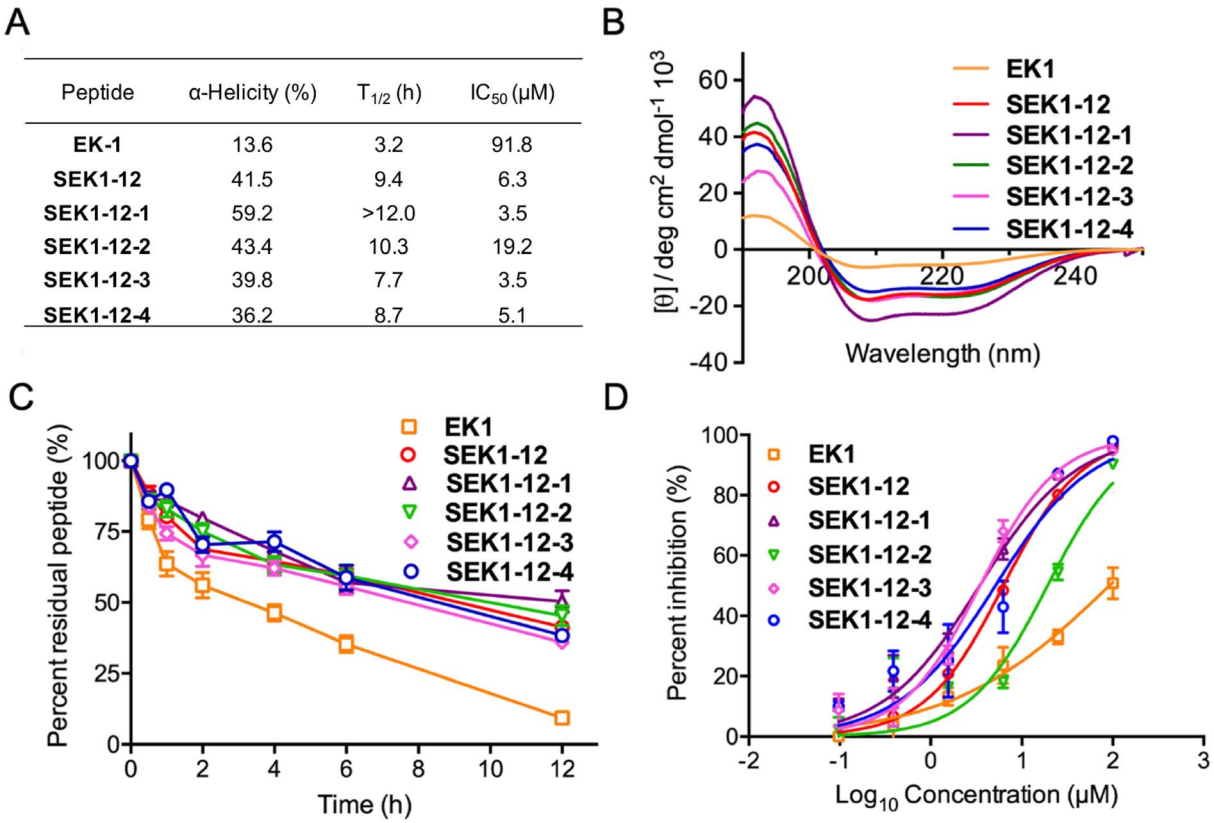

Fig. 4 The combinations of E_7-E_7, E_7-Z_7, Z_7-Z_7, Z_7-E_7 were applied to anti-SARS-CoV-2 peptides, thus generating geometry-specific stapled peptides. (A) Sequence diagram of the stapled peptides, and α-helical, half-life in chymotrypsin and IC_{50} anti-SARS-Cov-2 values. (B) The secondary structure of EK1 and its stapled peptides were analyzed by CD. It was proved that SEK1-12-1 of E_7-E_7 combination has the highest helical content among all peptides. (C) Protease stability of stapled peptides. The 0.5 ng mL^{-1} α-chymotrypsin was co-incubated with peptides, and the remaining peptide percent was monitored by analytic HPLC. (D) Live SARS-Cov-2 infection assay *in vitro*. The peptides of different concentrations were co-incubated with monolayer Vero-E6 cells, followed by the addition of SARS-CoV-2. Data are shown as the mean ± SEM of three independent experiments.

can enhance the helical stability of stapled peptides.[50] For validating the role of the introduced α-methyl and cyclobutyl groups of the stapled peptides in helical stabilization, we synthesized another stapled peptide counterpart without the α-methyl group, termed SEK1-12-5, and determined its helical content through experimental and theoretical calculations (Fig. S2†). The helicity of SEK1-12-5 was 33.8%, which was lower than 41.5% of SEK1-12 and 59.2% of SEK1-12-1. Notably, the helical contents of the geometry-specific hydrocarbon stapled peptides exhibited a significant difference, ranging from 36.2% to 59.2%. Among them, SEK1-12-1 (E_7-E_7) exhibited the highest helicity, approximately 1.5-fold that of SEK-1-12. These results indicated that the geometry-specific hydrocarbon stapling strategy could improve the helicity of linear peptides and classic hydrocarbon stapled peptides. More importantly, consistent with the theoretical calculation results, this improvement effect can be more pronounced than classical all-hydrocarbon stapling when properly paired E_7 and E_7 residues participated. Subsequently, α-chymotrypsin was incubated with these stapled peptides to evaluate its protease stability (Fig. 4C). 95% of the linear peptide quickly degraded after approximately 12 h of exposure, with a half-life of 3 h (E_7-E_7). In sharp contrast, all the stapled peptides exhibited obviously enhanced proteolytic stability, of which more than half SEK1-12-1 remained intact even after 12 h of exposure. This remarkable proteolytic stability was similar to that of previously reported cyclobutene-bearing cyclopeptides.[51]

To verify the antiviral activity of these peptides, we tested their inhibitory activity against live SARS-CoV-2 in a Biosafety Level 3 (BSL-3) facility at the Second Military Medical University (Fig. 4D). It was demonstrated that all the peptides were capable of inhibiting the replication of SARS-CoV-2 in a dose-dependent manner and the stapled peptides exhibited improved inhibitory activity than the original peptide EK1. Of note, except for SEK1-12-2, geometry-specific hydrocarbon stapled peptides exhibit better inhibitory activity than classical stapled peptides, indicating another effective stapling structure in SARS-CoV-2 peptide inhibitor development.

Conclusions

In this study, we have designed and efficiently obtained two unique cyclobutane-bearing conformationally restricted and olefin-terminated amino acids, termed E_7 and Z_7. Using E_7 and/or Z_7 as a paired combination, four kinds of geometry-specific

stapled peptides could be generated with the aid of the RCM reaction by *in silico* and on-resin experiments, of which the $\mathbf{E}_7$-$\mathbf{E}_7$ combination initiated stapling reaction was proven to be optimal. Targeting the spike protein HR1 domain of SARS-CoV-2 as a template peptide, we designed four geometry-specific hydrocarbon stapled peptides and also proved that SEK1-12-1 with $\mathbf{E}_7$-$\mathbf{E}_7$ combination exhibited the highest helical content using the combined quantum and molecular mechanics. Furthermore, SEK1-12-1 indeed exhibited the most stable helical conformation, the best proteolytic stability and thus the best anti-SARS-CoV-2 HR1 inhibitory activities. To sum up, our developed cyclobutane-bearing conformationally restricted anchoring residues with novel structure diversity were highly compatible with SPPS and RCM-mediated stapling chemistry. The generated geometry-specific hydrocarbon stapled peptide triggered from the $\mathbf{E}_7$-$\mathbf{E}_7$ combination was proven to be advantageous to the classic stapled counterpart in helical stabilization. In this regard, this methodology possesses great potential to expand the scope and structural diversity of the existing peptide stapling strategy. And thorough applications of this novel method into biologically active peptides are underway in our laboratory.

Data availability

All supporting data are provided in the ESI.†

Author contributions

BBC, HGH, XL and CL conceived and designed the study. BBC, CL, WC, FG, YZ, LL and DB performed the experiments. HGH, AH and LL helped with study design, and edited the manuscript. XL, BBC and CL wrote the paper. All authors read and approved the manuscript.

Conflicts of interest

The authors claim that the researchers in this study have no conflicts of interest.

Acknowledgements

This work was supported by the National Key R&D Program of China no. 2021YFC2100201 (to HH), the National Nature Science Foundation of China no. 22077078 (to HH), and the Shanghai Rising-Star Program (to XL).

Notes and references

1 J. F. Rual, K. Venkatesan, T. Hao, T. Hirozane-Kishikawa, A. Dricot, N. Li, G. F. Berriz, F. D. Gibbons, M. Dreze, N. Ayivi-Guedehoussou, N. Klitgord, C. Simon, M. Boxem, S. Milstein, J. Rosenberg, D. S. Goldberg, L. V. Zhang, S. L. Wong, G. Franklin, S. Li, J. S. Albala, J. Lim, C. Fraughton, E. Llamosas, S. Cevik, C. Bex, P. Lamesch, R. S. Sikorski, J. Vandenhaute, H. Y. Zoghbi, A. Smolyar, S. Bosak, R. Sequerra, L. Doucette-Stamm, M. E. Cusick, D. E. Hill, F. P. Roth and M. Vidal, *Nature*, 2005, **437**, 1173–1178.
2 T. L. Nero, C. J. Morton, J. K. Holien, J. Wielens and M. W. Parker, *Nat. Rev. Cancer*, 2014, **14**, 248–262.
3 V. Azzarito, K. Long, N. S. Murphy and A. J. Wilson, *Nat. Chem.*, 2013, **5**, 161–173.
4 L. D. Walensky and G. H. Bird, *J. Med. Chem.*, 2014, **57**, 6275–6288.
5 J. L. Nishikawa, A. Boeszoermenyi, L. A. Vale-Silva, R. Torelli, B. Posteraro, Y. J. Sohn, F. Ji, V. Gelev, D. Sanglard, M. Sanguinetti, R. I. Sadreyev, G. Mukherjee, J. Bhyravabhotla, S. J. Buhrlage, N. S. Gray, G. Wagner, A. M. Naar and H. Arthanari, *Nature*, 2016, **530**, 485–489.
6 K. H. Khoo, C. S. Verma and D. P. Lane, *Nat. Rev. Drug Discovery*, 2014, **13**, 217–236.
7 M. Wade, Y. C. Li and G. M. Wahl, *Nat. Rev. Cancer*, 2013, **13**, 83–96.
8 D. E. Scott, A. R. Bayly, C. Abell and J. Skidmore, *Nat. Rev. Drug Discovery*, 2016, **15**, 533–550.
9 L. G. Milroy, T. N. Grossmann, S. Hennig, L. Brunsveld and C. Ottmann, *Chem. Rev.*, 2014, **114**, 4695–4748.
10 I. Petta, S. Lievens, C. Libert, J. Tavernier and K. De Bosscher, *Mol. Ther.*, 2016, **24**, 707–718.
11 M. Rosell and J. Fernandez-Recio, *Expert Opin. Drug Discovery*, 2018, **13**, 327–338.
12 G. J. B. Philippe, D. J. Craik and S. T. Henriques, *Drug Discovery Today*, 2021, **26**, 1521–1531.
13 L. Wang, N. Wang, W. Zhang, X. Cheng, Z. Yan, G. Shao, X. Wang, R. Wang and C. Fu, *Signal Transduction Targeted Ther.*, 2022, **7**, 48.
14 K. Fosgerau and T. Hoffmann, *Drug Discovery Today*, 2015, **20**, 122–128.
15 S. K. Dubey, S. Parab, N. Dabholkar, M. Agrawal, G. Singhvi, A. Alexander, R. A. Bapat and P. Kesharwani, *Drug Discovery Today*, 2021, **26**, 931–950.
16 X. Li, S. Chen, W. D. Zhang and H. G. Hu, *Chem. Rev.*, 2020, **120**, 10079–10144.
17 R. Zhao, P. Shi, J. B. Cui, C. Shi, X. X. Wei, J. Luo, Z. Xia, W. W. Shi, Y. Zhou, J. Tang, C. Tian, M. Meininghaus, D. Bierer, J. Shi, Y. M. Li and L. Liu, *Angew. Chem., Int. Ed.*, 2023, **62**, e202216365.
18 Q. Qu, S. Gao, F. Wu, M. G. Zhang, Y. Li, L. H. Zhang, D. Bierer, C. L. Tian, J. S. Zheng and L. Liu, *Angew. Chem., Int. Ed.*, 2020, **59**, 6037–6045.
19 H. K. Cui, Y. Guo, Y. He, F. L. Wang, H. N. Chang, Y. J. Wang, F. M. Wu, C. L. Tian and L. Liu, *Angew. Chem., Int. Ed.*, 2013, **52**, 9558–9562.
20 R. S. Harrison, N. E. Shepherd, H. N. Hoang, G. Ruiz-Gomez, T. A. Hill, R. W. Driver, V. S. Desai, P. R. Young, G. Abbenante and D. P. Fairlie, *Proc. Natl. Acad. Sci. U. S. A.*, 2010, **107**, 11686–11691.
21 A. d. D. Araujo, J. Lim, K. C. Wu, Y. Xiang, A. C. Good, R. Skerlj and D. P. Fairlie, *J. Med. Chem.*, 2018, **61**, 2962–2972.
22 S. A. Kawamoto, A. Coleska, X. Ran, H. Yi, C. Y. Yang and S. Wang, *J. Med. Chem.*, 2012, **55**, 1137–1146.

23 N. J. Agard, J. A. Prescher and C. R. Bertozzi, *J. Am. Chem. Soc.*, 2004, **126**, 15046–15047.
24 Y. H. Lau, Y. Wu, M. Rossmann, B. X. Tan, P. de Andrade, Y. S. Tan, C. Verma, G. J. McKenzie, A. R. Venkitaraman, M. Hyvçnen and D. R. Spring, *Angew. Chem., Int. Ed.*, 2015, **54**, 15410–15413.
25 S. Learte-Aymami, C. Vidal, A. Gutierrez-Gonzalez and J. L. Mascarenas, *Angew. Chem., Int. Ed.*, 2020, **59**, 9149–9154.
26 A. A. Vinogradov, Z. N. Choo, K. A. Totaro and B. L. Pentelute, *Org. Lett.*, 2016, **18**, 1226–1229.
27 X. Li, W. D. Tolbert, H. G. Hu, N. Gohain, Y. Zou, F. Niu, W. X. He, W. Yuan, J. C. Su, M. Pazgier and W. Lu, *Chem. Sci.*, 2019, **10**, 1522–1530.
28 B. Li, Z. Wan, H. Zheng, S. Cai, H. W. Tian, H. Tang, X. Chu, G. He, D. S. Guo, X. S. Xue and G. Chen, *J. Am. Chem. Soc.*, 2022, **144**, 10080–10090.
29 N. Georgakopoulos, S. Talapatra, D. Dikovskaya, S. Dayalan Naidu, M. Higgins, J. Gatliff, A. Ayhan, R. Nikoloudaki, M. Schaap, K. Valko, F. Javid, A. T. Dinkova-Kostova, F. Kozielski and G. Wells, *J. Med. Chem.*, 2022, **65**, 7380–7398.
30 H. Jo, N. Meinhardt, Y. Wu, S. Kulkarni, X. Hu, K. E. Low, P. L. Davies, W. F. DeGrado and D. C. Greenbaum, *J. Am. Chem. Soc.*, 2012, **134**, 17704–17713.
31 F. Zhang, O. Sadovski, S. J. Xin and G. A. Woolley, *J. Am. Chem. Soc.*, 2007, **129**, 14154–14155.
32 X. Zheng, Z. Li, W. Gao, X. Meng, X. Li, L. Y. P. Luk, Y. Zhao, Y. H. Tsai and C. Wu, *J. Am. Chem. Soc.*, 2020, **142**, 5097–5103.
33 Z. Bai, C. Cai, W. Sheng, Y. Ren and H. Wang, *Angew. Chem., Int. Ed.*, 2020, **59**, 14686–14692.
34 X. Li, Y. Zou and H. G. Hu, *Chinese Chem. Lett.*, 2018, **29**, 1088–1092.
35 C. E. Schafmeister, J. Po and G. L. Verdine, *J. Am. Chem. Soc.*, 2000, **122**, 5891–5892.
36 M. Feng, J. Q. Jin, L. Xia, T. Xiao, S. Mei, X. Wang, X. Huang, J. Chen, M. Liu, C. Chen, S. Rafi, A. X. Zhu, Y. X. Feng and D. Zhu, *Sci. Adv.*, 2019, **5**, eaau5240.
37 Y. S. Chang, B. Graves, V. Guerlavais, C. Tovar, K. Packman, K. H. To, K. A. Olson, K. Kesavan, P. Gangurde, A. Mukherjee, T. Baker, K. Darlak, C. Elkin, Z. Filipovic, F. Z. Qureshi, H. Cai, P. Berry, E. Feyfant, X. E. Shi, J. Horstick, D. A. Annis, A. M. Manning, N. Fotouhi, H. Nash, L. T. Vassilev and T. K. Sawyer, *Proc. Natl. Acad. Sci. U. S. A.*, 2013, **110**, 3445–3454.
38 M. L. Stewart, E. Fire, A. E. Keating and L. D. Walensky, *Nat. Chem. Biol.*, 2010, **6**, 595–601.
39 Y. S. Chang, B. Graves, V. Guerlavais, C. Tovar, K. Packman, K. H. To, K. A. Olson, K. Kesavan, P. Gangurde, A. Mukherjee, T. Baker, K. Darlak, C. Elkin, Z. Filipovic, F. Z. Qureshi, H. Cai, P. Berry, E. Feyfant, X. E. Shi, J. Horstick, D. A. Annis, A. M. Manning, N. Fotouhi, H. Nash, L. T. Vassilev and T. K. Sawyer, *Proc. Natl. Acad. Sci. U. S. A.*, 2013, **110**, 3445–3454.
40 Y. Lai, G. Fois, J. R. Flores, M. J. Tuvim, Q. Zhou, K. Yang, J. Leitz, J. Peters, Y. Zhang, R. A. Pfuetzner, L. Esquivies, P. Jones, M. Frick, B. F. Dickey and A. T. Brunger, *Nature*, 2022, **603**, 949–956.
41 Y. Wu, Y. H. Li, X. Li, Y. Zou, H. L. Liao, L. Liu, Y. G. Chen, D. Bierer and H. G. Hu, *Chem. Sci.*, 2017, **8**, 7368–7373.
42 A. N. Tkachenko, D. S. Radchenko, P. K. Mykhailiuk, S. Afonin, A. S. Ulrich and I. V. Komarov, *Angew. Chem., Int. Ed.*, 2013, **52**, 6504–6507.
43 O. M. Michurin, S. Afonin, M. Berditsch, C. G. Daniliuc, A. S. Ulrich, I. V. Komarov and D. S. Radchenko, *Angew. Chem., Int. Ed.*, 2016, **55**, 14595–14599.
44 O. M. Michurin, K. Tolmachova, S. Afonin, O. Babii, S. L. Grage, A. S. Ulrich, I. V. Komarov and D. S. Radchenko, *Eur. J. Org. Chem.*, 2018, **2018**, 3826–3833.
45 A. N. Tkachenko, P. K. Mykhailiuk, S. Afonin, D. S. Radchenko, V. S. Kubyshkin, A. S. Ulrich and I. V. Komarov, *Angew. Chem., Int. Ed.*, 2013, **52**, 1486–1489.
46 J. Li, Z. Zhang, J. Gu, R. Amini, A. G. Mansfield, J. Xia, D. White, H. D. Stacey, J. C. Ang, G. Panesar, A. Capretta, C. D. M. Filipe, K. Mossman, B. J. Salena, J. B. Gubbay, C. Balion, L. Soleymani, M. S. Miller, D. Yamamura, J. D. Brennan and Y. Li, *J. Am. Chem. Soc.*, 2022, **144**, 23465–23473.
47 B. Oberfeld, A. Achanta, K. Carpenter, P. Chen, N. M. Gilette, P. Langat, J. T. Said, A. E. Schiff, A. S. Zhou, A. K. Barczak and S. Pillai, *Cell*, 2020, **181**, 954–954.
48 S. Xia, M. Liu, C. Wang, W. Xu, Q. Lan, S. Feng, F. Qi, L. Bao, L. Du, S. Liu, C. Qin, F. Sun, Z. Shi, Y. Zhu, S. Jiang and L. Lu, *Cell Res.*, 2020, **30**, 343–355.
49 S. Xia, L. Yan, W. Xu, A. S. Agrawal, A. Algaissi, C. K. Tseng, Q. Wang, L. Du, W. Tan, I. A. Wilson, S. Jiang, B. Yang and L. Lu, *Sci. Adv.*, 2019, **5**, eaav4580.
50 C. E. Schafmeister, J. Po and G. L. Verdine, *J. Am. Chem. Soc.*, 2000, **122**, 5891–5892.
51 T. Miura, T. R. Malla, C. D. Owen, A. Tumber, L. Brewitz, M. A. McDonough, E. Salah, N. Terasaka, T. Katoh, P. Lukacik, C. Strain-Damerell, H. Mikolajek, M. A. Walsh, A. Kawamura, C. J. Schofield and H. Suga, *Nat. Chem.*, 2023, **15**, 998–1005.